Effect of Model Polycyclic Aromatic Compounds on the Coalescence of Water-in-Oil Emulsion Droplets

Cuiying Jian[†,‡], *Qingxia Liu*[‡], *Hongbo Zeng*[‡,*], *and Tian Tang*[†,*]

[†]Department of Mechanical Engineering and

[‡]Department of Chemical and Material Engineering,

University of Alberta, Edmonton, AB, Canada

[*]Corresponding author;

Phone: +1-780-492-1044. Fax: +1-780-492-2881. E-mail: hongbo.zeng@ualberta.ca (H.Z.)

Phone: +1-780-492-5467. Fax: +1-780-492-2200. E-mail: tian.tang@ualberta.ca (T.T.)

ABSTRACT: A series of molecular dynamics simulations were performed to investigate the effect of polycyclic aromatic compounds (PACs) on the coalescence of two water droplets in oil (i.e. n-heptane and toluene). Our simulations revealed that in both solvents the presence of PACs can significantly hinder the coalescence or even completely prevent it. Detailed structural and kinetic analysis provided insights into the underlying mechanisms for the coalescence inhibition. In n-heptane, regardless of their concentration, the PAC molecules formed an adsorption layer on the water droplets which, if the concentration is sufficiently high, is able to introduce strong steric hindrance and shield the water-water interaction. While the formation of an adsorption layer was also observed in toluene at sufficiently high PAC concentration, the prevention of coalescence at relatively low concentration is mainly driven by the un-adsorbed, free-floating PAC molecules in the bulk toluene. The simulation results reported here fully agree with our previous experimental observations and well interpreted the experimental results from the atomic level.

1. INTRODUCTION

Water-in-oil (W/O) emulsions are present in many industrial processes.[1-5] While they are greatly desired in certain areas, such as food and cosmetics processing,[1,2] the emulsions formed during oil production can impose deleterious effects on facility maintenance, water recycling, and efficient processing of petroleum compounds.[3-5] Particularly, due to the presence of interfacially active components, W/O emulsions can be stabilized during petroleum processing, consequently it is extremely difficult to collect water via coalescence for recycling.[5] One such interfacially active component is the asphaltene fraction, which are polycyclic aromatic compounds (PACs) with heteroatoms, and have been generally believed to stabilize the W/O emulsions.[6-11] Therefore, a significant amount of work in literature has been dedicated to probing the adsorption behaviors of PAC molecules onto water droplets, as well as the resultant adverse effect on coalescence.[6, 7, 12-18]

Over the past two decades, much effort has been devoted to investigating the effect of asphaltenes on emulsion stability.[6,7,12-14,15-20] It has been suggested[6,7,16,19,21, 22] that the protective layer, formed by asphaltene molecules on the water/oil interface, is responsible for stabilizing the emulsions. Despite the progress made in experiments, mechanistic understanding at the atomistic level is still under debates. For example, in literature there is no conclusive agreement on whether the adsorption is in the form of asphaltene monomers or aggregates, and whether the orientation of the polyaromatic cores of the adsorbed asphaltenes is parallel or perpendicular with respect to the water/oil interface.[7,13-18] While with the help of small angle X-ray and neutron scattering structural organization of asphaltenes at the interface can be characterized, such as in the work of Barre and co-authors[23,24] as well as Verruto et al.[25], direct visualization of the adsorption process at molecular level and the resultant molecular arrangements are still

inaccessible by the existing experimental techniques. Motivated by this, computational approaches, for instance, molecular dynamics (MD) simulations, which can provide atomistic visualizations, have been employed to investigate the behaviors of PAC molecules at water/oil interfaces.[26-43]

Adopting representative PACs, computational studies performed on flat water/oil interfaces have revealed that the type of solvent, molecular architecture and functional groups of the PAC, and its concentration can all affect the adsorption behaviors of asphaltenes.[37-41] For instance, it was observed that in n-heptane, PAC molecules were prone to adsorption and did so in an aggregated state, while they preferred to stay in the bulk toluene phase due to the better solubility in toluene.[38, 41] Furthermore, in the work of Ruiz-Morales and Mullins,[40] the relative orientation of PAC molecules at the interface were suggested to be affected by the presence of oxygen functionality in the PAC molecules. While these studies helped visualizing the adsorption phenomena, W/O emulsions in these works were mimicked by flat interfaces between water and organic solvent, which prevented the study of coalescence of water droplets. Only in two recent MD works were spherical water droplets employed to investigate the adsorption behaviors of PAC molecules.[42, 43]

Firstly, in the work of Liu et al.,[42] one water droplet was suspended in toluene and model asphaltene molecules were randomly distributed near the droplet surface. It was observed that at the concentration studied (205.3 g/L), the PAC molecules ($C_{47}H_{55}NS$) adsorbed on the water droplets were in an aggregated state with their polyaromatic cores parallel with one another but perpendicular to the interface. Motivated by this, our recent work,[43] for the first time, addressed the size effects of water droplets on the adsorption of PAC molecules. Initially, representative PAC molecules were dispersed in an organic solvent phase (n-heptane or toluene), which also

contained a single water droplet. By simulating water droplets of different radii, it was found[43] that while the size effect in toluene is only prominent when the concentration of PAC molecules is sufficiently high, in n-heptane the curvature of the PAC aggregates formed on the droplet surface is sensitive to the size of the water droplet.

Despite the above efforts, to date there has not been any reports where the coalescence of water droplets in the presence of PAC molecules is directly simulated. To fill this gap, in this work, a series of MD simulations were performed on systems containing two water droplets in oil with PAC molecules. While droplets in experiments are in excess of 1-10 μm in size, aggregation/coalescence of droplets starts at nanometer scales, where the detailed mechanisms may not be adequately captured by experiments.[44] In this context, MD simulations can be employed to investigate the molecular organizations and evolution of oil/water interfaces during coalescence. For our current work here, the droplets were initially separated by a certain distance in an organic solvent phase (n-heptane or toluene), which allowed us to directly probe the dynamics of coalescence, the effect of PAC molecules and the underlying mechanisms.

2. SIMULATION METHODS

Violanthrone-79 (VO-79, $C_{50}H_{48}O_4$, Figure 1) was adopted as a model PAC, which has a central polyaromatic core and two side chains. Oil phase was represented, respectively, by n-heptane or toluene as PAC molecules have distinct solubilities in these two solvents (n-heptane: "bad" solvent; toluene: "good solvent").[45,46] It is important to note that "real" asphaltenes are a complex class of molecules and there are large variations in their composition from one reservoir to another. Consequently, it is impossible to expect a single type of model compound to represent the full features of asphaltenes. However VO-79 shares structural similarities with the

island-type asphaltenes proposed in literature,[47] and its oxygen content (9.0%) is relatively close to that of the asphaltene fractions stabilizing W/O emulsions (4.42%-5.54%).[48,49] It and similar molecules have been widely employed in literature as a representative model for studying asphaltene properties.[50-54]

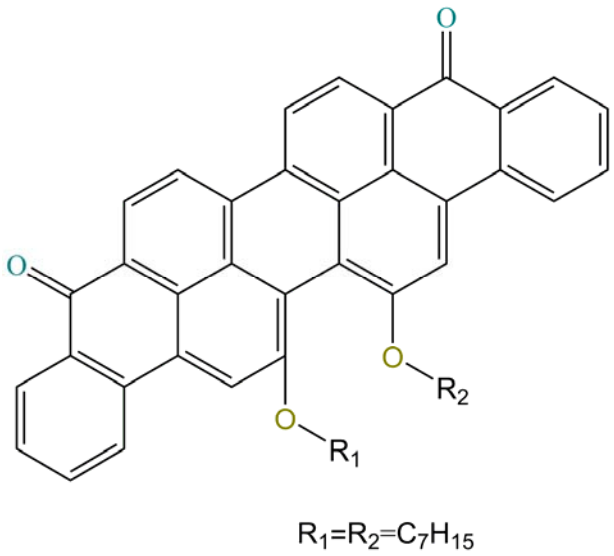

Figure 1. Chemical structure of the VO-79 compound.

2.1. Systems Simulated. To probe the effect of VO-79 on the coalescence of water droplets, 5 systems were constructed, each containing either n-heptane or toluene as the organic solvent phase, two water droplets, and a certain number of VO-79 molecules. Two reference systems in the absence of VO-79 were also simulated. Details of these systems are summarized in Table 1.

Table 1. Details of the simulated systems

system	initial box size (nm^3)	water box size (nm^3)	no. of water boxes	no. of n-heptane molecules	no. of toluene molecules	no. of PAC molecules	PAC conc. (mM)
HEP	$28 \times 14 \times 14$	$5 \times 5 \times 5$	2	19780			
HEP-144	$28 \times 14 \times 14$	$5 \times 5 \times 5$	2	18034		144	43.6
HEP-432	$28 \times 14 \times 14$	$5 \times 5 \times 5$	2	16879		432	131
TOL	$28 \times 14 \times 14$	$5 \times 5 \times 5$	2		27847		
TOL-144	$28 \times 14 \times 14$	$5 \times 5 \times 5$	2		25598	144	43.6
TOL-432	$28 \times 14 \times 14$	$5 \times 5 \times 5$	2		24046	432	131
TOL-24	$28 \times 14 \times 14$	$5 \times 5 \times 5$	2		27487	24	7.26

The first system in Table 1, namely HEP, contains n-heptane as the organic solvent with two water droplets in the absence of VO-79. In constructing the initial configurations, the water droplets were first introduced using two cubic water boxes, each of dimension $5 \times 5 \times 5$ nm^3. These two water boxes were packed side by side into a simulation box of dimension $28 \times 14 \times 14$ nm^3 (see Figure 2a). Then the rest of the box was filled with n-heptane molecules. During equilibration, the two water boxes quickly formed spherical water droplets each of radius ~ 3.10 nm. The next two systems in Table 1 (system HEP-144 and HEP-432) also contain n-heptane as the organic solvent but with the presence of VO-79. For these two systems, to construct the initial configuration, 12 or 36 VO-79 molecules were arranged to form an ordered array occupying each facet of each water box, resulting in a total of $12 \times 6 \times 2 = 144$ VO-79 molecules in system HEP-144, and $36 \times 6 \times 2 = 432$ VO-79 molecules in system HEP-432 (Figure 2b). The different numbers of VO-79 molecules in these two systems allow us to investigate the effect of VO-79 concentration on the coalescence of water droplets.

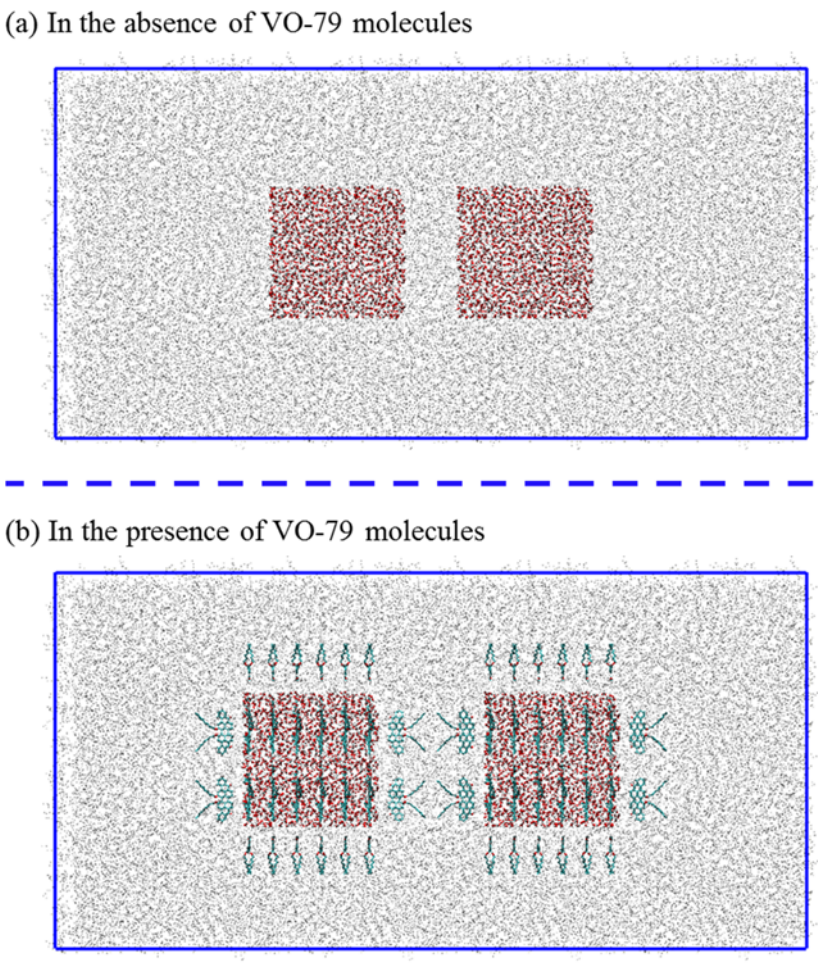

Figure 2. Initial configurations (side views) for systems: (a) HEP and TOL; and (b) HEP-144 and TOL-144. PAC molecules are mainly colored cyan and water molecules colored red; gray points represent organic solvents. Systems HEP-432, TOL-432 and TOL-24 share a similar configuration with (b), but have different numbers of PAC molecules.

Similar initial configurations were adopted in systems TOL, TOL-144, and TOL-432, which had toluene as the solvent. Furthermore, we performed an additional simulation in toluene, TOL-24 in Table 1. In this system, initially, a very small number (2) of VO-79 molecules were arranged to occupy each facet of each water droplet. The reason for performing this simulation is that due to the good solubility of VO-79 in toluene, coalescence of water droplets is absent even

in system TOL-144 (details presented in section 3). This suggests that a wider range of concentrations may be needed to obtain a complete picture of the effect of VO-79. Therefore we further lowered the concentration of VO-79 in toluene.

2.2. Simulation Details. The topologies for VO-79, toluene and n-heptane were created and validated in our previous work,[34, 35, 41,55] and directly adopted here. For water molecules, a simple-point-charge (SPC) model[56] was used, which has been extensively tested in literature for interfacial studies.[39, 57, 58]

All simulations were performed using the MD package GROMACS[59-62] with periodic boundary conditions applied. For each system, static structure optimization was first performed to ensure that the maximum force is less than 1000.0 kJ/(mol × nm). Then full dynamics simulation was conducted in NPT ensemble at 1 bar and 300 K for 50 ns. It is important to point out that due to the intrinsic limitation of MD simulations, while our simulation time is not directly comparable to experiments, the studies here still provide us with insights into the initial stage of droplet coalescence (details provided in section 3).

During dynamics simulations, the pressure and temperature was controlled, respectively, using a Parrinello-Rahman barostat[63] and a velocity rescaling thermostat.[64] The latter is based on correctly producing the probability distribution of kinetic energy under constant temperature, and thus is an accurate method.[64] Throughout the dynamics simulation, the SETTLE algorithm[65] to constrain the intra-molecular bonds in water molecules, the LINCS algorithm[66] to constrain all bonds in other molecules, and a time step of 2 fs were used. For all simulations, full electrostatics was treated by particle-mesh Ewald method,[67] and van der Waals interactions were evaluated by a cutoff approach with a shift potential, both having a cutoff distance of 1.4 nm. Appropriate

post-processing programs available in GROMACS were used for trajectory analysis and VMD[68] for visualization.

3. RESULTS AND DISCUSSION

To track the occurrence of coalescence, we monitored the distance between the centers of mass (COMs) of the two water droplets, namely $d_{COM}(\mathrm{nm})$, inside each system. Here for each droplet, the COM was determined by averaging the positions of all water molecules it contained in the initial configuration, and will hereafter be referred to as the "droplet COM". When the two droplets coalesce, water molecules become well mixed, leading to $d_{COM}(\mathrm{nm}) = 0$. Figure 3 plots d_{COM} for all the systems studied in this work. As can be seen, in the absence of VO-79 (systems HEP and TOL), d_{COM} quickly decays to zero (within 5 ns), corresponding to coalescence. This agrees well with the phenomena observed in our recent experimental measurements between two water droplets in toluene or heptane using atomic force microscope (AFM) droplet probe technique.[11] In contrast, with the presence of VO-79, the decay of d_{COM} either is retarded (in systems HEP-144 and TOL-24) or diminishes (in all the other 3 systems). In systems TOL-144 and TOL-432 (Figure 3b), d_{COM} even shows an overall increasing trend, suggesting that the two droplets move away from each other during the simulation course. Again, this observation agrees well with our AFM force measurements between two W/O emulsion drops, and force measurements between asphaltene layers using surface forces apparatus (SFA), in asphaltene-toluene solutions.[10, 11, 69] To understand these phenomena as well as the underlying mechanisms, below, we presented a detailed investigation on the simulated systems containing VO-79.

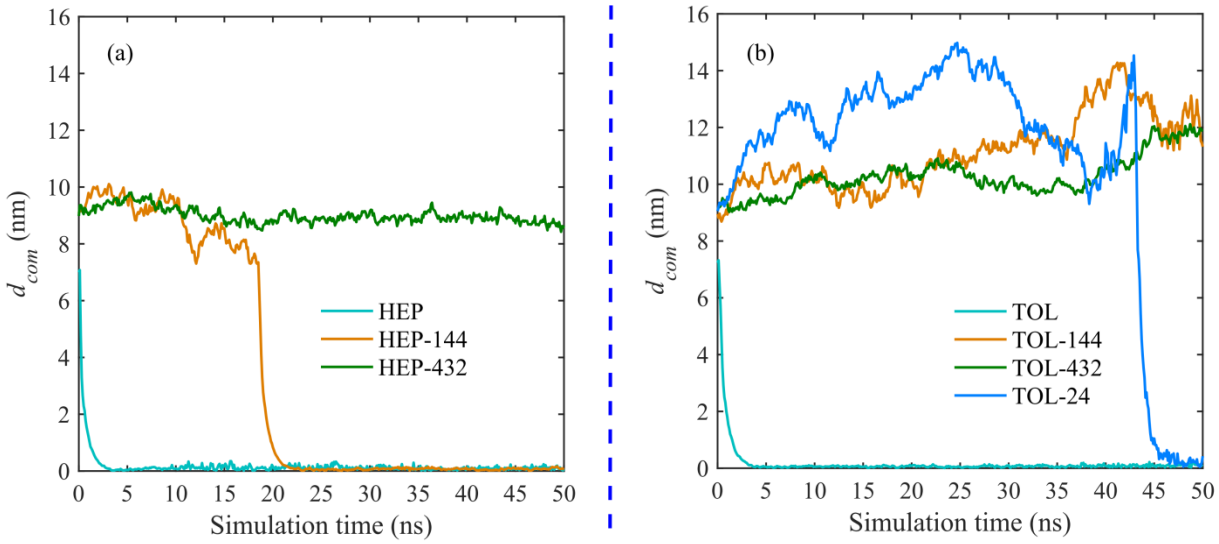

Figure 3. (a) d_{COM} in systems HEP, HEP-144 and HEP-432, and (b) d_{COM} in systems TOL, TOL-144, TOL-432 and TOl-24, versus simulation time.

3.1. Effects of PACs on Coalescence in *n*-Heptane. From Figure 3a, coalescence of water droplets is observed in system HEP-144 but not in system HEP-432. To understand this, we first monitored the motions of the two droplets in system HEP-144 (Figure 4). The right panel in Figure 4 plots the radial distribution functions (RDFs) for the distance (r (nm)) between the COM of each VO-79's polyaromatic core and the COM of the water phase. Here the COM of the water phase (referred to as "water COM" hereafter) is calculated by averaging the positions of all water molecules in the system, i.e. from both droplets. Each RDF plot was generated by considering the average over a certain time span: (b) 0 to 1 ns, (d) 15 to 20 ns, and (f) 45 to 50 ns, so together they provide information on how the system evolves with time. The snapshots in the left panel of Figure 4 are representative configurations corresponding, respectively, to the three time spans in the right panel.

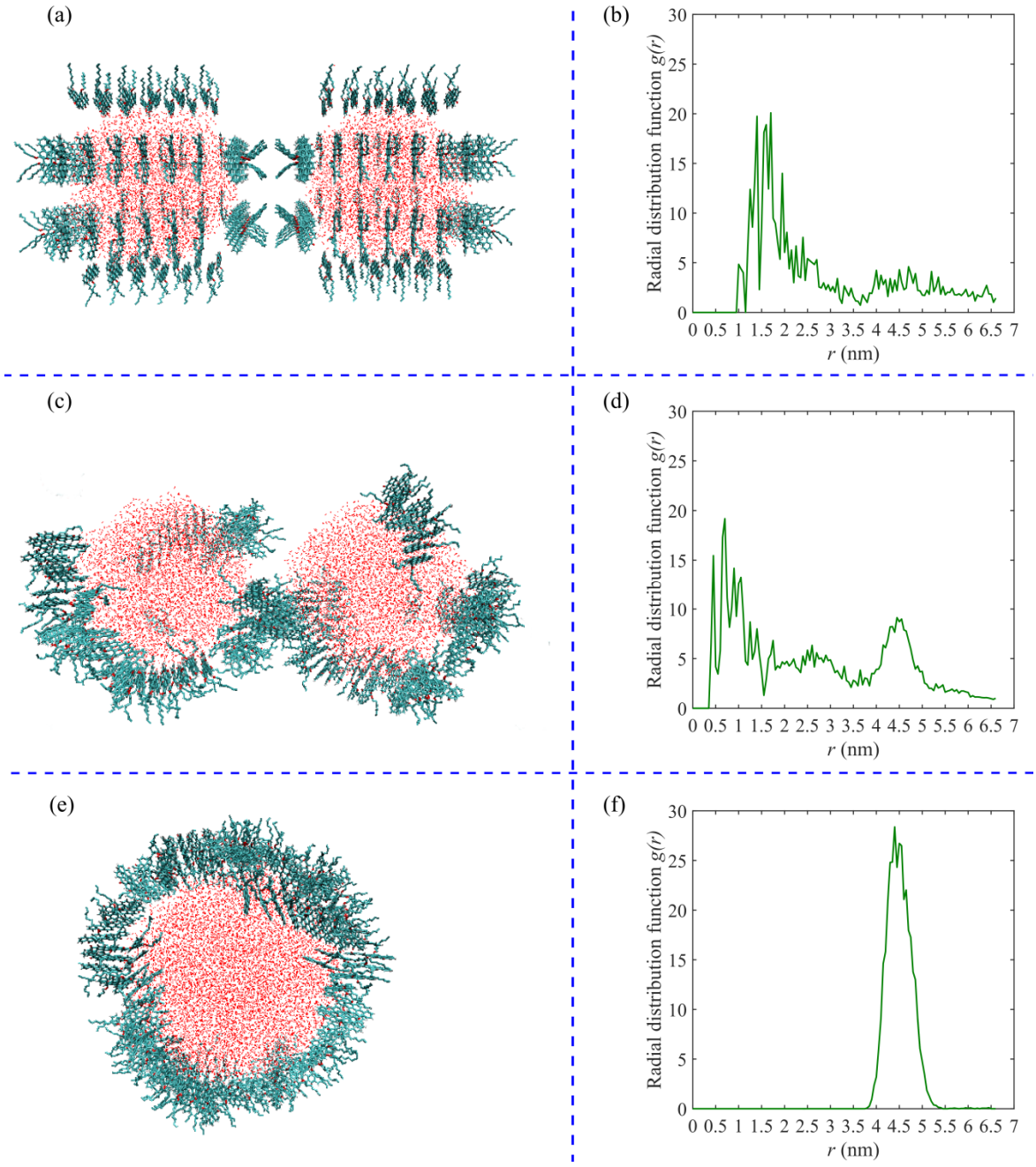

Figure 4. Representative configurations in system HEP-144 (left panel), and the corresponding RDFs of VO-79 molecules around the water COM (right panel): (a-b) initial stage, averaged over 0 to 1 ns for (b); (c-d) middle stage, averaged over 15 to 20 ns for (d); and (e-f) final stage, averaged over 45 to 50 ns for (f). In the left panel, water molecules are colored red with VO-79 molecules colored cyan; n-heptane molecules are removed for clarity.

Initially, the two droplets were separated with $d_{COM} = 9$ nm (Figure 3a), each surrounded by 72 VO-79 molecules (Figure 4a). In this scenario, the water COM is located at the middle point of the line connecting the individual droplet COMs. Since the radius of each water droplet is ~3.10 nm, the distance between the water COM and the surface of each water droplet, where VO-79 molecules are found, is $(9 - 3.10 \times 2)/2 = 1.40$ nm. Consistently, the most prominent peaks in the corresponding RDF (Figure 4b) are located at $r = 1.2 - 2$ nm.

As the simulation proceeded, the two droplets approached each other. Consequently, d_{COM} (Figure 3a) reduced from 9 nm (at 0 ns) to 8 nm (at ~15 ns), and continued to decrease between 15 ns and 20 ns. Meanwhile, initially separated VO-79 molecules began to form aggregates with parallel and closely stacked polyaromatic cores. As a result, they became localized on the droplet surfaces. This is evidenced in Figure 4c, where most VO-79 molecules are concentrated at the bottom of each droplet, with their cores being parallel with one another but perpendicular to the droplet surface. The orientations observed here is consistent with the experimental work of Andrews et al.,[70] where "edge-on" configuration was proposed for Violanthrone-78 (VO-78, structurally very similar to VO-79). However it should be mentioned that due to the diverse molecular structures real asphaltenes possess, they have also been reported in literature[16,70] to exhibit opposite configurations at oil/water or oil/solid interfaces, such as parallel to the interface. Nevertheless, regardless of the orientation, this localization observed on water droplets, together with the decreased d_{COM}, leads to an overall reduction in the distance between VO-79 molecules and the water COM. For instance, at $d_{COM} = 8$ nm, the most probable values of r would be close to $(8 - 3.10 \times 2)/2 = 0.90$ nm. Therefore compared to the initial stage (Figure 4b), the most prominent peaks in the RDF now (Figure 4d) appear at shorter distances ($r = 0.4 - 1.2$ nm).

The aggregation and localization of VO-79 increased the area of uncovered (free) water surfaces (Figure 4c as compared to Figure 4a). Therefore direct contact can be formed between water molecules in the two droplets, which is necessary for initiating the coalescence. In return, the availability of free water surfaces also made it possible for the VO-79 aggregates to reposition themselves, thus facilitating the further deformation of each droplet. Consequently, coalescence was finally observed (Figure 4e), resulting in a combined droplet with radius ~3.91 nm. Furthermore, during the process of coalescence, VO-79 previously adsorbed on different droplets co-aggregated on the combined droplet. The RDF at the final stage has the most prominent peaks at $r = \sim$4.4 nm (Figure 4f), which is close to the radius of the combined droplet. It is worth pointing out that compared to system HEP, the coalescence was delayed in system HEP-144 (Figure 3a), since it required time for the adsorbed VO-79 molecules to reposition and co-aggregate.

In contrast, the dynamics of the droplets in the late stage of the simulation is different at a higher concentration of VO-79. This is shown in Figure 5 where the representative configurations and the associated RDFs are presented for system HEP-432. In the initial stage (0 to 1 ns), the configuration and RDF for system HEP-432 (Figures 5a-b) are similar to those for system HEP-144 (Figures 4a-b). As system HEP-432 evolved, the two droplets started to approach each other. Correspondingly, the prominent peaks in the RDF (Figure 5d) appear at shorter distances compared to Figure 5b, similar to the change observed from Figure 4b to Figure 4d. Also, the aggregated VO-79 molecules still have their polyaromatic cores being parallel with one another and perpendicular to the water surface. Despite these similarities, unlike in system HEP-144, each water droplet in system HEP-432 is almost fully covered by VO-79 aggregates,

leaving hardly any free water surfaces (Figure 5c). Accordingly, significant differences are observed in the final stage between the two systems (Figure 4 e-f vs. Figure 5 e-f).

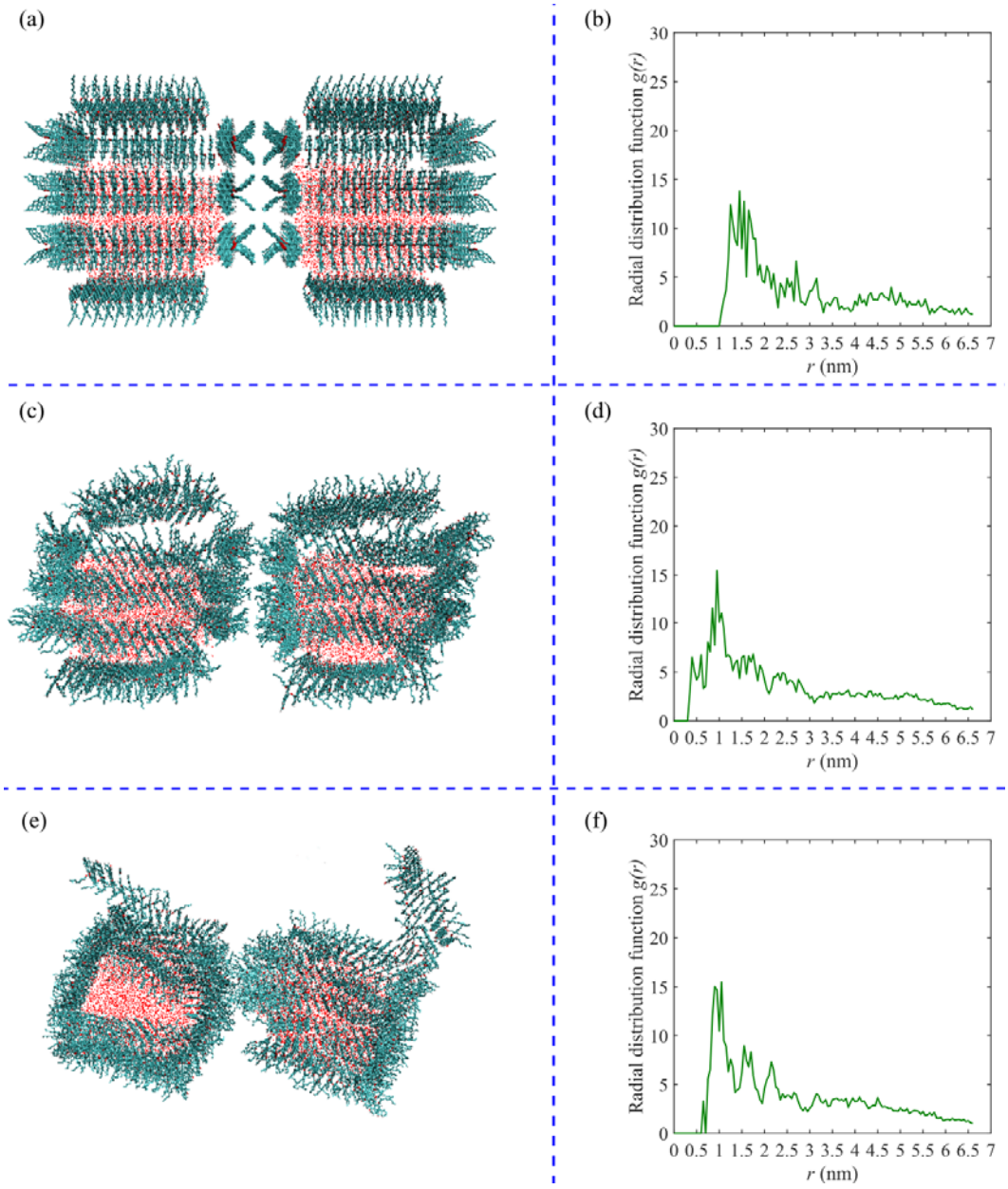

Figure 5. Representative configurations in system HEP-432 (left panel), and the corresponding RDFs of VO-79 molecules around the water COM (right panel): (a-b) initial stage, averaged over 0-1 ns for (b); (c-d) middle stage, averaged over 15 to 20 ns for (d); and (e-f) final stage, averaged over 45 to 50 ns for (f). In the left panel, water molecules are colored red with VO-79 molecules colored cyan; *n*-heptane molecules are removed for clarity.

Firstly, in Figure 5e, some VO-79 molecules have lost direct contact with water, and are only adsorbed to the droplet through other VO-79 molecules. This can be attributed to the lack of free water surface to accommodate its interaction with all 432 VO-79 molecules. For the same reason, while the fully covered water droplets are bridged by the side chains of VO-79, there is no direct contact between the two water droplets, and of course no coalescence. Correspondingly, compared to Figure 4f, the prominent peaks in the RDF at the end stage (Figure 5f) still appear at relatively short distances ($r = 0.5 - 1.5$ nm). From these observations, it is clear that at sufficiently high concentrations, while VO-79 molecules could bridge the two droplets, they brought in strong steric hindrance and shielded water-water interaction, thus introducing resistance to coalescence. This indicates that in n-heptane the two droplets are stabilized by VO-79 after its concentration reaches a certain threshold. Indeed, it has been observed, in our previous experiments,[10,11] that water-in-heptane emulsion droplets in the presence of asphaltenes tended to be stable against coalescence but adhere to each other (see Figure 6). While the size of the droplets employed in our simulation is on the order of nm, which is considerably smaller than the size in experiments, the phenomena observed qualitatively agree with each other.

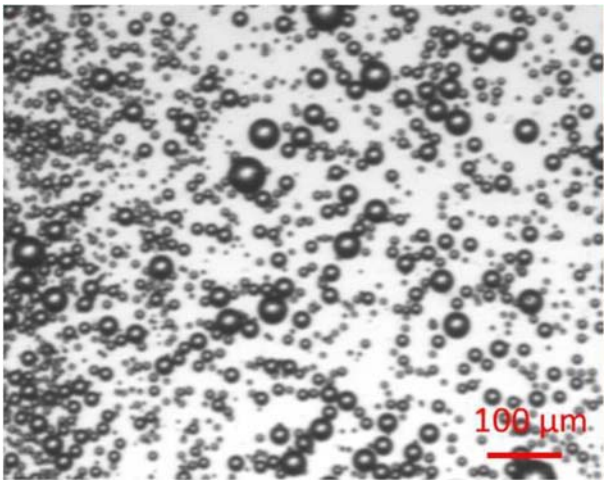

Figure 6. Stable water-in-heptane emulsion. The emulsion was prepared by adding abundant n-heptane to a pre-prepared water-in-toluene emulsion with 0.3wt% asphaltene, and the image was taken on suspension in the supernatant layer. Full experimental details can be found in ref[10, 11] .

3.2. Effects of PACs on Coalescence in Toluene. Unlike in n-heptane, coalescence were absent in both systems TOL-144 and TOL-432. In fact, with the presence of VO-79, coalescence of water droplets is only observed in system TOL-24 at ~45 ns, where the VO-79 concentration is very low. Therefore it is of interest to investigate how the presence of VO-79 can affect the coalescence of water droplets in toluene, as well as how the effect may differ from that in n-heptane.

In literature, it has been observed[38, 41] that unlike the evident adsorption in n-heptane, VO-79 molecules prefer to stay in the bulk toluene phase. For our systems simulated here, to probe the adsorption dynamics, we first calculated the number of VO-79 molecules adsorbed to each droplet in system TOL-144. To do so, the two droplets were labeled as Droplet 1 and Droplet 2 respectively. Next, two index groups were built, one containing Droplet 1 and all the 144 VO-79 molecules, and the other containing Droplet 2 and all the 144 VO-79 molecules. Let

us first consider the index group containing Droplet 1. During the course of the simulation, some of the VO-79 molecules may adsorb onto Droplet 1, either through direct contact, or via indirect attachment by stacking with other VO-79 molecules. We call the water droplet along with the adsorbed VO-79 molecules a cluster. The number of molecules in this cluster, including water and VO-79, was calculated using a single linkage algorithm with cutoff distance = 0.5 nm and denoted by n_1. Meanwhile we also monitored the number (n_2) of water molecules involved in this cluster. Hence the number of VO-79 molecules adsorbed to Droplet 1 is given by $n = n_1 - n_2$. In the same way, we can obtain the number of VO-79 molecules adsorbed to Droplet 2, and these data are plotted in Figure 7a.

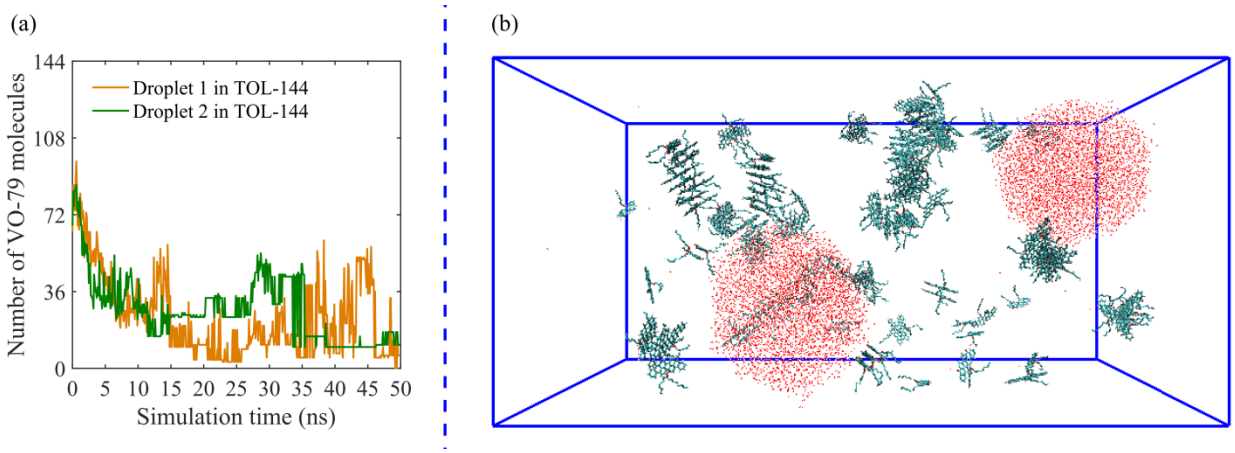

Figure 7. For system TOL-144: (a) number of VO-79 molecules adsorbed to each water droplet, and (b) representative configuration in the final stage. In (b), blue lines represent the simulation box, water molecules are colored red and VO-79 molecules are in cyan; toluene molecules are removed for clarity.

Clearly, in Figure 7a, the two curves render an overall decreasing trend, indicating that the VO-79 molecules initially adsorbed to the droplets detached from them and moved into the bulk toluene phase. Indeed, most VO-79 molecules are distributed in the bulk in the end stage of

the simulation (Figure 7b). That is, consistent with our previous report,[43] the adsorption in toluene is more reversible than that in n-heptane, a result from the better solubility of PAC molecules in toluene.[45, 46] Although a protective layer is not formed around the water droplets at this concentration, the un-adsorbed, free-floating VO-79 molecules, in monomer or aggregated form, are dispersed in toluene and thus can create barriers for the water droplets to diffuse and collide. Indeed, as shown in Figure 3b, in system TOL-144, d_{COM} between the two droplets actually shows an overall increasing trend, indicating further separation of the droplets with the presence of VO-79 molecules. It should be pointed out that this unusual observation is likely induced by the very high bulk concentration employed here (see section 3.3 for detailed rationale of choosing such high concentrations), which, coupled with periodic boundary conditions, can introduce a very crowded bulk phase, resulting in the apparent "repulsion" between water droplets. Nevertheless, the phenomena observed here could correspond to the repulsion effect detected between two approaching water-in-oil drops in the presence of asphaltenes by droplet probe AFM, and between two approaching mica surfaces in asphaltene-toluene or PAC-in-toluene solutions using a surface forces apparatus (SFA), in our previous experiments. [10, 11,69,71]

Compared to system TOL-144, the bulk VO-79 concentration in system TOL-432 is increased by a factor of 3. Using the same method described above, we monitored the number of VO-79 molecules adsorbed to each droplet in system TOL-432, and this is plotted in Figure 8a. The first observation made from Figure 8a is that the overall decreasing trend observed in system TOL-144 (Figure 7a) is now absent. Instead, the two curves show significant step-wise fluctuations, especially in the late stage of the simulation. Further examination of Figure 8a reveals that the two curves frequently switch between two values: one close to ~432, corresponding to the total amount of VO-79 molecules, and the other close to ~216, roughly the

amount of initially adsorbed VO-79 molecules on each droplet. To understand this, it is necessary to examine the final configurations formed in system TOL-432.

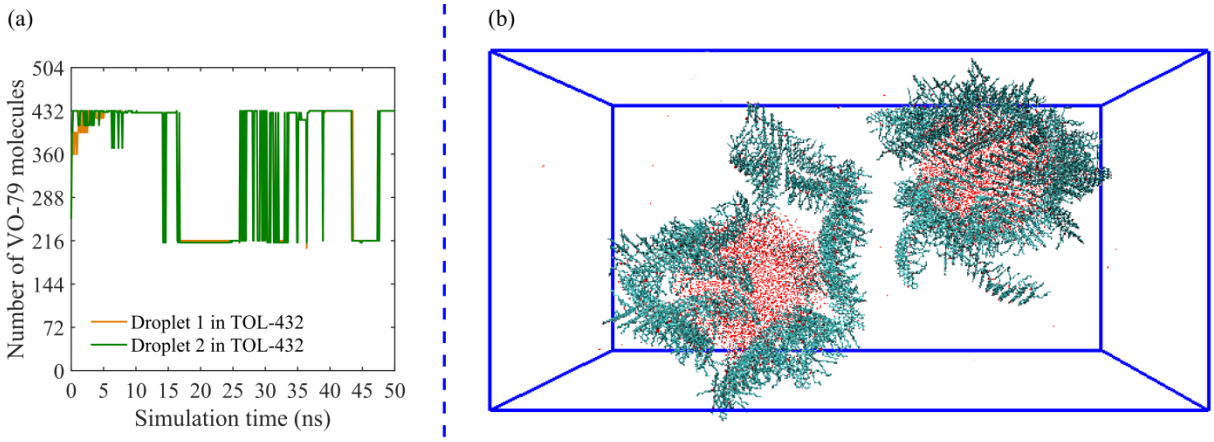

Figure 8. For system TOL-432: (a) number of VO-79 molecules adsorbed to each water droplet, and (b) representative configuration in the final stage. In (b), blue lines represent the simulation box, water molecules are colored red and VO-79 molecules are in cyan; toluene molecules are removed for clarity.

As shown in Figure 8b, at this high concentration both droplets are coated with aggregated VO-79 molecules. Correspondingly in Figure 8a, at least ~216 molecules are adsorbed to each water droplet. Due to this strong adsorption, similar to system HEP-432, while the two water droplets are prevented from forming direct contact, they can be bridged by the side chains of VO-79 molecules. When such a bridge is formed, the 216 molecules that were adsorbed to Droplet 2 are now also adsorbed to Droplet 1, leading to the increase of n_1 from 216 to 432. The same occurs to n_2. On the other hand, due to the relatively large solubility of VO-79 in toluene,[45, 46] the bridge is much less stable than that in n-heptane. Therefore, it frequently breaks, and when this happens, d_{COM} in Figure 3b increases, and the number of VO-79 molecules adsorbed to each droplet reduces to its initial value (~216).

The above comparisons between systems TOL-144 and TOL-432 have demonstrated that while coalescence is hindered by the un-adsorbed, free-floating VO-79 molecules at low concentration, at high concentration the effect of VO-79 on coalescence is two-fold. Firstly, the protective layer formed by the adsorbed VO-79 introduces resistance to coalescence. Secondly, while the adsorbed VO-79 molecules can bridge the droplets, they also have strong attractions with the solvent toluene. As a result they can drag the coated water droplets to diffuse in the bulk toluene phase, and thus cause the separation of droplets.

While unlike in simulations, detailed locations of asphaltenes may not be readily observable in experiments, the macroscopic effect of concentration/solvent found in experiments can be correlated with the atomistic details from simulations. For example, the above simulation results, especially observed in system TOL-432, qualitatively agree with our recent micropipette tests where almost no coalescence was observed between two water-in-toluene emulsion drops at high asphaltene concentrations, under which some asphaltenes migrated to the oil/water interface and formed a "protective" interfacial layer.[10] In addition, the simulation results also agree with our recent force measurements, using AFM droplet probe technique, between two water droplets in toluene having asphaltenes at the oil/water interfaces.[11] In the AFM force measurements, repulsive forces were measured when the two W/O emulsion drops with interfacial asphaltenes approached each other, while adhesion was detected during separation if certain compressive load were applied after two emulsion drops were in contact.[11] Furthermore, the results reported here can help to interpret our previous results on SFA force measurements, where a longer-range repulsion was observed during the approach of two mica surfaces (adsorbed with asphaltenes) in toluene solutions of high asphaltene concentrations.[69]

3.3 Implications on Droplet Coalescence As presented above, in both systems HEP-432 and TOL-432 (high concentration), VO-79 molecules form an adsorption layer on the water droplets. This finding directly supports the experimental postulation[6, 7,16,19] that the protective layer, formed by PAC molecules on the droplet surface, is responsible for stabilizing W/O emulsions. In addition, our current work provides structural details regarding this adsorption layer. For instance, most of the adsorbed VO-79 molecules are in an aggregated form with parallel stacking of their polyaromatic cores. These polyaromatic cores are prone to interact with water and hence are perpendicular to the droplet surface, while the side chains reside in the exterior. The information on these molecular structures, which is not accessible by current experimental techniques, can help to propose appropriate means to remove or destroy the protective layer formed by PAC molecules.

More interestingly, within the time scale employed here, our simulations revealed that in "good" solvents such as toluene, the diffusion of PAC molecules also introduced obstacles to the coalescence of water droplets. This is particularly important at relatively low concentration where adsorption is absent but coalescence is still prevented. Having the understanding of different mechanisms driving coalescence inhibition is essential if one is to control the occurrence of coalescence during industrial processing (e.g. via the use of different solvent).

Finally, we mention that the bulk concentrations employed in our simulations are much higher than those usually employed in experiments. For instance, our lowest bulk concentration is 7.26 mM (system TOL-24), where coalescence was observed in toluene. Contrarily, in experiments, such as in the work of Nenningsland et al.,[7] it was reported that coalescence of water droplets could be hindered by PAC molecules at a concentration of 0.08 mM in xylene. Since toluene and xylene have similar molecular structures, the distinct difference should be

attributed to the fact that "local concentrations" rather than "bulk concentrations" determine the occurrence of coalescence. As discussed in our previous work,[43] in experiments where coalescence is absent, the local concentration of PAC molecules near the water droplets can be much higher than the homogenized bulk concentration.[72] Therefore, to mimic the high local concentration in experiments, it is actually required to adopt higher bulk concentrations in MD simulations. Specifically, in the work of Andrews et al.,[70] the area per VO-78 molecule on the interface was calculated to be 0.65 nm^2. In our systems HEP-432 and TOL-432, the total surface area of the two droplets is $2 \times 4 \times \pi \times (3.10)^2 = 242$ nm^2, and hence area per VO-79 molecule on the interface is $242/432 = 0.56$ nm^2, close to the surface concentration calculated by Andrews et al.[70] On the other hand, they correspond to drastically different bulk concentrations, 93.3 mg/mL in our simulations vs. 0.1 mg/mL in the experiments of Andrews et al.[70]

Finally, it should be emphasized that while our droplet sizes (~nm) are orders of magnitude smaller than those naturally encountered in petroleum processing (~μm), they are comparable to the sizes (~nm) of nanoemulsions stabilized by surfactants in experiments.[73,74] Therefore the discussion presented here can provide valuable information for preparing desired nanoemulsions. For instance, it can help with predicting the stability of nanoemulsions under different solvent and concentration conditions.

4. CONCLUSIONS

In this work, we employed all-atom MD simulations to investigate the effect of PAC molecules on the coalescence of water droplets in n-heptane and toluene. It was found that in both solvents, the presence of PAC molecules can either delay or completely prevent the coalescence. In n-heptane, irrespective of the concentrations, the adsorption of PAC molecules leads to the

formation of a protective layer on the water droplet. At sufficiently high concentrations, the steric hindrance and shielding introduced by the adsorption layer can prevent the water droplets from coalescence. In contrast, due to the better solubility of PAC molecules in toluene, their effect on coalescence is also different. At low concentrations, the PAC molecules prefer to stay in the bulk toluene phase, and these un-adsorbed free-floating PAC molecules can create barriers for water droplets to collide and to coalesce. With increasing concentration, like in n-heptane, a protective layer is also formed by PAC molecules on the water droplets in toluene. However, these adsorbed PAC molecules can drag the coated water droplets to diffuse in the bulk toluene, thus bringing additional obstacles to coalescence. These findings fully agree with our previous experimental observations and clarify the fundamental mechanism for the effects of PAC molecules on droplet coalescence in different solvents and at different concentrations.

ACKNOWLEDGEMENTS

We acknowledge the computing resources and technical support from Western Canada Research Grid (WestGrid). Financial support from the Natural Science and Engineering Research Council (NSERC) of Canada, Canadian Centre for Clean Coal/Carbon and Mineral Processing Technologies (C^5MPT), Alberta Innovates – Energy and Environment Solutions (AI-EES) and Nexen Energy ULC is gratefully acknowledged.

References

(1) Ghosh, S.; Rousseau, D. Fat Crystals and Water-in-Oil Emulsion Stability. *Curr. Opin. Colloid Interface Sci.* **2011**, *16*, 421-431.

(2) Yoneyama, T.; Yamaguchi, M.; Tobe, S.; Nanba, T.; Ishiwatari, M.; Toyoda, H.; Nakamura, S.; Kumano, Y.; Takata, S.; Ito, H. Water-in-Oil Emulsion Type Cosmetics. U.S. Patent 5,015,469, May 14, **1991**.

(3) Mouraille, O.; Skodvin, T.; Sjöblom, J.; Peytavy, J. Stability of Water-in-Crude Oil Emulsions: Role Played by the State of Solvation of Asphaltenes and by Waxes. *J. Dispersion Sci. Technol.* **1998**, *19*, 339-367.

(4) Spiecker, P. M.; Gawrys, K. L.; Trail, C. B.; Kilpatrick, P. K. Effects of Petroleum Resins on Asphaltene Aggregation and Water-in-Oil Emulsion Formation. *Colloids Surf., A* **2003**, *220*, 9-27.

(5) Kilpatrick, P. K. Water-in-Crude Oil Emulsion Stabilization: Review and Unanswered Questions. *Energy Fuels* **2012**, *26*, 4017-4026.

(6) McLean, J. D.; Kilpatrick, P. K. Effects of Asphaltene Solvency on Stability of Water-in-Crude-Oil Emulsions. *J. Colloid Interface Sci.* **1997**, *189*, 242-253.

(7) Nenningsland, A. L.; Gao, B.; Simon, S.; Sjöblom, J. Comparative Study of Stabilizing Agents for Water-in-Oil Emulsions. *Energy Fuels* **2011**, *25*, 5746-5754.

(8) Groenzin, H.; Mullins, O. C. Asphaltene Molecular Size and Structure. *J. Phys. Chem. A* **1999**, *103*, 11237-11245.

(9) Speight, J. Petroleum Asphaltenes-Part 1: Asphaltenes, Resins and the Structure of Petroleum. *Oil Gas Sci. Technol.* **2004**, *59*, 467-477.

(10) Zhang, L.; Shi, C.; Lu, Q.; Liu, Q.; Zeng, H. Probing Molecular Interactions of Asphaltenes in Heptol using a Surface Forces Apparatus: Implications on Stability of Water-in-Oil Emulsions. *Langmuir* **2016**, *32*, 4886-4895.

(11) Shi, C.; Zhang, L.; Xie, L.; Lu, X.; Liu, Q.; He, J.; Mantilla, C. A.; van den Berg, Frans GA; Zeng, H. Surface Interaction of Water-in-Oil Emulsion Droplets with Interfacially Active Asphaltenes. *Langmuir* **2017**, *33*, 1265–1274.

(12) McLean, J. D.; Kilpatrick, P. K. Effects of Asphaltene Aggregation in Model heptane–toluene Mixtures on Stability of Water-in-Oil Emulsions. *J. Colloid Interface Sci.* **1997**, *196*, 23-34.

(13) Nordgård, E. L.; Sørland, G.; Sjöblom, J. Behavior of Asphaltene Model Compounds at W/O Interfaces. *Langmuir* **2009**, *26*, 2352-2360.

(14) Bi, J.; Yang, F.; Harbottle, D.; Pensini, E.; Tchoukov, P.; Simon, S.; Sjöblom, J.; Dabros, T.; Czarnecki, J.; Liu, Q. Interfacial Layer Properties of a Polyaromatic Compound and its Role in Stabilizing Water-in-Oil Emulsions. *Langmuir* **2015**, *31*, 10382-10391.

(15) Rane, J. P.; Harbottle, D.; Pauchard, V.; Couzis, A.; Banerjee, S. Adsorption Kinetics of Asphaltenes at the oil–water Interface and Nanoaggregation in the Bulk. *Langmuir* **2012**, *28*, 9986-9995.

(16) Rane, J. P.; Pauchard, V.; Couzis, A.; Banerjee, S. Interfacial Rheology of Asphaltenes at oil–water Interfaces and Interpretation of the Equation of State. *Langmuir* **2013**, *29*, 4750-4759.

(17) Pauchard, V.; Rane, J. P.; Zarkar, S.; Couzis, A.; Banerjee, S. Long-Term Adsorption Kinetics of Asphaltenes at the Oil–Water Interface: A Random Sequential Adsorption Perspective. *Langmuir* **2014**, *30*, 8381-8390.

(18) Rane, J. P.; Zarkar, S.; Pauchard, V.; Mullins, O. C.; Christie, D.; Andrews, A. B.; Pomerantz, A. E.; Banerjee, S. Applicability of the Langmuir Equation of State for Asphaltene Adsorption at the Oil–Water Interface: Coal-Derived, Petroleum, and Synthetic Asphaltenes. *Energy Fuels* **2015**, *29*, 3584-3590.

(19) Yang, F.; Tchoukov, P.; Pensini, E.; Dabros, T.; Czarnecki, J.; Masliyah, J.; Xu, Z. Asphaltene Subfractions Responsible for Stabilizing Water-in-Crude Oil Emulsions. Part 1: Interfacial Behaviors. *Energy Fuels* **2014**, *28*, 6897-6904.

(20) Gao, S.; Moran, K.; Xu, Z.; Masliyah, J. Role of Naphthenic Acids in Stabilizing Water-in-Diluted Model Oil Emulsions. *J. Phys. Chem. B* **2010**, *114*, 7710-7718.

(21) Sjöblom, J.; Mingyuan, L.; Christy, A. A.; Gu, T. Water-in-Crude-Oil Emulsions from the Norwegian Continental Shelf 7. Interfacial Pressure and Emulsion Stability. *Colloids Surf.* **1992**, *66*, 55-62.

(22) Acevedo, S.; Escobar, G.; Gutiérrez, L. B.; Rivas, H.; Gutiérrez, X. Interfacial Rheological Studies of Extra-Heavy Crude Oils and Asphaltenes: Role of the Dispersion Effect of Resins in the Adsorption of Asphaltenes at the Interface of Water-in-Crude Oil Emulsions. *Colloids Surf., A* **1993**, *71*, 65-71.

(23) Jestin, J.; Simon, S.; Zupancic, L.; Barré, L. A Small Angle Neutron Scattering Study of the Adsorbed Asphaltene Layer in Water-in-Hydrocarbon Emulsions: Structural Description Related to Stability. *Langmuir* **2007**, *23*, 10471-10478.

(24) Jestin, J.; Simon, S.; Zupancic, L.; Barré, L. A Small Angle Neutron Scattering Study of the Adsorbed Asphaltene Layer in Water-in-Hydrocarbon Emulsions: Structural Description Related to Stability. *Langmuir* **2007**, *23*, 10471-10478.

(25) Verruto, V. J.; Kilpatrick, P. K. Water-in-Model Oil Emulsions Studied by Small-Angle Neutron Scattering: Interfacial Film Thickness and Composition. *Langmuir* **2008**, *24*, 12807-12822.

(26) Headen, T. F.; Boek, E. S.; Skipper, N. T. Evidence for Asphaltene Nanoaggregation in Toluene and Heptane from Molecular Dynamics Simulations. *Energy Fuels* **2009**, *23*, 1220-1229.

(27) Boek, E. S.; Yakovlev, D. S.; Headen, T. F. Quantitative Molecular Representation of Asphaltenes and Molecular Dynamics Simulation of their Aggregation. *Energy Fuels* **2009**, *23*, 1209-1219.

(28) Headen, T. F.; Boek, E. S. Molecular Dynamics Simulations of Asphaltene Aggregation in Supercritical Carbon Dioxide with and without Limonene. *Energy Fuels* **2010**, *25*, 503-508.

(29) Teklebrhan, R. B.; Ge, L.; Bhattacharjee, S.; Xu, Z.; Sjöblom, J. Probing Structure–Nanoaggregation Relations of Polyaromatic Surfactants: A Molecular Dynamics Simulation and Dynamic Light Scattering Study. *J. Phys. Chem. B* **2012**, *116*, 5907-5918.

(30) Sedghi, M.; Goual, L.; Welch, W.; Kubelka, J. Effect of Asphaltene Structure on Association and Aggregation using Molecular Dynamics. *J. Phys. Chem. B* **2013**, *117*, 5765-5776.

(31) Frigerio, F.; Molinari, D. A Multiscale Approach to the Simulation of Asphaltenes. *Comput. Theor. Chem.* **2011**, *975*, 76-82.

(32) Kuznicki, T.; Masliyah, J. H.; Bhattacharjee, S. Molecular Dynamics Study of Model Molecules Resembling Asphaltene-Like Structures in Aqueous Organic Solvent Systems. *Energy Fuels* **2008**, *22*, 2379-2389.

(33) Jian, C.; Tang, T.; Bhattacharjee, S. Probing the Effect of Side Chain Length on the Aggregation of a Model Asphaltene using Molecular Dynamics Simulations. *Energy Fuels*, **2013**, *27*, 2057–2067.

(34) Jian, C.; Tang, T.; Bhattacharjee, S. Molecular Dynamics Investigation on the Aggregation of Violanthrone78-Based Model Asphaltenes in Toluene. *Energy Fuels* **2014**, *28*, 3604–3613 .

(35) Jian, C.; Tang, T. One-Dimensional Self-Assembly of Poly-Aromatic Compounds Revealed by Molecular Dynamics Simulations. *J. Phys. Chem. B* **2014***, 118,* 12772–12780.

(36) Jian, C.; Tang, T. Molecular Dynamics Simulations Reveal Inhomogeneity-Enhanced Stacking of Violanthrone-78-Based Polyaromatic Compounds in n-Heptane–Toluene Mixtures. *J. Phys. Chem. B* **2015**, *119*, 8660-8668.

(37) Gao, F.; Xu, Z.; Liu, G.; Yuan, S. Molecular Dynamics Simulation: The Behavior of Asphaltene in Crude Oil and at the Oil/Water Interface. *Energy Fuels* **2014**, *28*, 7368-7376.

(38) Teklebrhan, R. B.; Ge, L.; Bhattacharjee, S.; Xu, Z.; Sjöblom, J. Initial Partition and Aggregation of Uncharged Polyaromatic Molecules at the Oil-Water Interface: A Molecular Dynamics Simulation Study. *J. Phys. Chem. B* **2014**, *118,* 1040–1051.

(39) Kuznicki, T.; Masliyah, J. H.; Bhattacharjee, S. Aggregation and Partitioning of Model Asphaltenes at Toluene− Water Interfaces: Molecular Dynamics Simulations. *Energy Fuels* **2009**, *23*, 5027-5035.

(40) Ruiz-Morales, Y.; Mullins, O. C. Coarse-Grained Molecular Simulations to Investigate Asphaltenes at the Oil–Water Interface. *Energy Fuels* **2015**, *29*, 1597-1609.

(41) Jian, C.; Poopari, M. R.; Liu, Q.; Zerpa, N.; Zeng, H.; Tang, T. Reduction of Water/Oil Interfacial Tension by Model Asphaltenes: The Governing Role of Surface Concentration. *J. Phys. Chem. B* **2016**, *120,* 5646–5654.

(42) Liu, J.; Zhao, Y.; Ren, S. Molecular Dynamics Simulation of Self-Aggregation of Asphaltenes at an Oil/Water Interface: Formation and Destruction of the Asphaltene Protective Film. *Energy Fuels* **2015**, *29*, 1233-1242.

(43) Jian, C.; Zeng, H.; Liu, Q.; Tang, T. Probing the Adsorption of Polycyclic Aromatic Compounds Onto Water Droplets using Molecular Dynamics Simulations. *J. Phys. Chem. C* **2016**, *120*, 14170-14179.

(44) Rezaei, H.; Amjad-Iranagh, S.; Modarress, H. Self-Accumulation of Uncharged Polyaromatic Surfactants at Crude Oil–Water Interface: A Mesoscopic DPD Study. *Energy Fuels* **2016**, *30*, 6626-6639.

(45) Speight, J. G.; Long, R. B.; Trowbridge, T. D. Factors Influencing the Separation of Asphaltenes from Heavy Petroleum Feedstocks. *Fuel* **1984**, *63*, 616-620.

(46) Yarranton, H. W.; Alboudwarej, H.; Jakher, R. Investigation of Asphaltene Association with Vapor Pressure Osmometry and Interfacial Tension Measurements. *Ind. Eng. Chem. Res.* **2000**, *39*, 2916-2924.

(47) Schuler, B.; Meyer, G.; Peña, D.; Mullins, O. C.; Gross, L. Unraveling the Molecular Structures of Asphaltenes by Atomic Force Microscopy. *J. Am. Chem. Soc.* **2015**, *137*, 9870-9876.

(48) Subramanian, S.; Simon, S.; Gao, B.; Sjöblom, J. Asphaltene Fractionation Based on Adsorption Onto Calcium Carbonate: Part 1. Characterization of Sub-Fractions and QCM-D Measurements. *Colloids Surf., A* **2016**, *495*, 136-148.

(49) Yang, F.; Tchoukov, P.; Dettman, H.; Teklebrhan, R. B.; Liu, L.; Dabros, T.; Czarnecki, J.; Masliyah, J.; Xu, Z. Asphaltene Subfractions Responsible for Stabilizing Water-in-Crude Oil Emulsions. Part 2: Molecular Representations and Molecular Dynamics Simulations. *Energy Fuels* **2015**, *29*, 4783-4794.

(50) Lopez-Linares, F. C., L; Gonzalez, M. S., C; Figueras, M. P., P Quinolin-65 and Violanthrone-79 as Model Molecules for the Kinetics of the Adsorption of C7 Athabasca Asphaltene on Macroporous Solid Surfaces. *Energy Fuels* **2006**, *20*, 2748.

(51) González, M. F.; Stull, C. S.; López-Linares, F.; Pereira-Almao, P. Comparing Asphaltene Adsorption with Model Heavy Molecules Over Macroporous Solid Surfaces. *Energy Fuels* **2007**, *21*, 234-241.

(52) Jarne, C.; Cebolla, V. L.; Membrado, L.; Le Mapihan, K.; Giusti, P. High-Performance Thin-Layer Chromatography using Automated Multiple Development for the Separation of Heavy Petroleum Products According to their Number of Aromatic Rings. *Energy Fuels* **2011**, *25*, 4586-4594.

(53) Hmoudah, M.; Nassar, N. N.; Vitale, G.; El-Qanni, A. Effect of Nanosized and Surface-Structural-Modified Nano-Pyroxene on Adsorption of Violanthrone-79. *RSC Advances* **2016**, *6*, 64482-64493.

(54) Zi, M.; Chen, D.; Ji, H.; Wu, G. Effects of Asphaltenes on the Formation and Decomposition of Methane Hydrate: A Molecular Dynamics Study. *Energy Fuels* **2016**, *30*, 5643-5650.

(55) Jian, C.; Tang, T.; Bhattacharjee, S. A Dimension Map for Molecular Aggregates. *J. Mol. Graph. Model.* **2015**, *58*, 10-15.

(56) Berendsen, H. J. C.; Postma, J. P. M.; van Gunsteren, W.; Hermans, J. Interaction Models for Water in Relation to Protein Hydration. In Intermolecular Forces; Pullmann, B., Ed.; D. Reidel Publishing Company: Dordrecht, The Netherlands, **1981**; pp 331– 342.

(57) Tieleman, D.; Berendsen, H. Molecular Dynamics Simulations of a Fully Hydrated Dipalmitoylphosphatidylcholine Bilayer with Different Macroscopic Boundary Conditions and Parameters. *J. Chem. Phys.* **1996**, *105*, 4871-4880.

(58) Zielkiewicz, J. Structural Properties of Water: Comparison of the SPC, SPCE, TIP4P, and TIP5P Models of Water. *J. Chem. Phys.* **2005**, *123*, 104501.

(59) Hess, B.; Kutzner, C.; van der Spoel, D.; Lindahl, E. GROMACS 4: Algorithms for Highly Efficient, Load-Balanced, and Scalable Molecular Simulation. *J. Chem. Theory Comput.* **2008**, *4*, 435-447.

(60) Van Der Spoel, D.; Lindahl, E.; Hess, B.; Groenhof, G.; Mark, A. E.; Berendsen, H. J. GROMACS: Fast, Flexible, and Free. *J. Comput. Chem.* **2005**, *26*, 1701-1718.

(61) Lindahl, E.; Hess, B.; Van Der Spoel, D. GROMACS 3.0: A Package for Molecular Simulation and Trajectory Analysis. *J. Mol. Model.* **2001**, *7*, 306-317.

(62) Berendsen, H. J.; van der Spoel, D.; van Drunen, R. GROMACS: A Message-Passing Parallel Molecular Dynamics Implementation. *Comput. Phys. Commun.* **1995**, *91*, 43-56.

(63) Parrinello, M.; Rahman, A. Polymorphic Transitions in Single Crystals: A New Molecular Dynamics Method. *J. Appl. Phys.* **1981**, *52*, 7182-7190.

(64) Bussi, G.; Donadio, D.; Parrinello, M. Canonical Sampling through Velocity-Rescaling. *J. Chem. Phys.* **2007**, *126,* 014101.

(65) Miyamoto, S.; Kollman, P. A. Settle: An Analytical Version of the SHAKE and RATTLE Algorithm for Rigid Water Models. *J. Comput. Chem.* **1992**, *13*, 952-962.

(66) Hess, B. P-LINCS: A Parallel Linear Constraint Solver for Molecular Simulation. *J J. Chem. Theory Comput.* **2008**, *4*, 116-122.

(67) Essmann, U.; Perera, L.; Berkowitz, M. L.; Darden, T.; Lee, H.; Pedersen, L. G. A Smooth Particle Mesh Ewald Method. *J. Chem. Phys.* **1995**, *103*, 8577.

(68) Humphrey, W.; Dalke, A.; Schulten, K. VMD: Visual Molecular Dynamics. *J. Mol. Graph.* **1996**, *14*, 33-38.

(69) Natarajan, A.; Kuznicki, N.; Harbottle, D.; Masliyah, J.; Zeng, H.; Xu, Z. Understanding Mechanisms of Asphaltene Adsorption from Organic Solvent on Mica. *Langmuir* **2014**, *30*, 9370-9377.

(70) Andrews, A. B.; McClelland, A.; Korkeila, O.; Demidov, A.; Krummel, A.; Mullins, O. C.; Chen, Z. Molecular Orientation of Asphaltenes and PAH Model Compounds in Langmuir− Blodgett Films using Sum Frequency Generation Spectroscopy. *Langmuir* **2011**, *27*, 6049-6058.

(71) Wang, J.; van der Tuuk Opedal, Nils; Lu, Q.; Xu, Z.; Zeng, H.; Sjöblom, J. Probing Molecular Interactions of an Asphaltene Model Compound in Organic Solvents using a Surface Forces Apparatus (SFA). *Energy Fuels* **2011**, *26*, 2591-2599.

(72) Grimes, B.; Dorao, C.; Simon, S.; Nordgård, E.; Sjöblom, J. Analysis of Dynamic Surfactant Mass Transfer and its Relationship to the Transient Stabilization of Coalescing liquid–liquid Dispersions. *J. Colloid Interface Sci.* **2010**, *348*, 479-490.

(73) Eley, D.; Hey, M.; Symonds, J. Emulsions of Water in Asphaltene-Containing Oils 1. Droplet Size Distribution and Emulsification Rates. *Colloids and surfaces* **1988**, *32*, 87-101.

(74) Peng, L.; Liu, C.; Kwan, C.; Huang, K. Optimization of Water-in-Oil Nanoemulsions by Mixed Surfactants. *Colloids Surf., A* **2010**, *370*, 136-142.

TOC Graphic

Polycyclic aromatic compounds inhibit water drop coalescence via two different mechanisms.